Published in final edited form as:
Carbohydr Polym. 2014 March 15; 103: 392–397. doi:10.1016/j.carbpol.2013.12.066.

Inulin isoforms differ by repeated additions of one crystal unit cell

Peter D. Cooper[a,b,*], **Thomas G. Barclay**[c], **Milena Ginic-Markovic**[c], **Andrea R. Gerson**[c], and **Nikolai Petrovsky**[a,d,#]

[a]Vaxine Pty Ltd, Flinders Medical Centre, Bedford Park, SA, Australia 5042

[b]Cancer Research Laboratory, Australian National University Medical School at The Canberra Hospital, Garran, ACT, Australia 2605; and the John Curtin School of Medical Research, The Australian National University, Acton, ACT, Australia 2601

[c]The Mawson Institute, University of South Australia, Mawson Lakes, SA, Australia 5095

[d]Department of Endocrinology, Flinders Medical Centre/Flinders University, Bedford Park, SA, Australia, 5042

Abstract

Inulin isoforms, especially delta inulin, are important biologically as immune activators and clinically as vaccine adjuvants. In exploring action mechanisms, we previously found regular increments in thermal properties of the seven-member inulin isoform series that suggested regular additions of some energetic structural unit. Because the previous isolates carried additional longer chains that masked defining ranges, these were contrasted with new isoform isolates comprising only inulin chain lengths defining that isoform. The new series began with 19 fructose units per chain (alpha-1 inulin), increasing regularly by 6 fructose units per isoform. Thus the 'energetic unit' equates to 6 fructose residues per chain. All isoforms showed indistinguishable X-ray diffraction patterns that were also identical with known inulin crystals. We conclude that an 'energetic unit' equates to one helix turn of 6 fructose units per chain as found in one unit cell of the inulin crystal. Each isoform chain comprised progressively more helix turns plus one additional fructose and glucose residues per chain.

Keywords

adjuvant; carbohydrate; inulin; isoform; polymorph; vaccine

[*]Corresponding author. Tel:+61-2-62319926; Fax: +61-8-82045987; peter.cooper@anu.edu.au.
[#]Author for proofs and reprints. Tel: +61-8-82044572; Fax: +61-8-82045987; nikolai.petrovsky@flinders.edu.au

Conflict of interest statement: P.C. and N.P. are employees or consultants of Vaxine Pty Ltd.

1. Introduction

Inulin is a versatile polysaccharide with many applications (Barclay, Ginic-Markovic, Cooper, & Petrovsky, 2010). Our interest lies in micro-particulate inulin (MPI) isoforms with demonstrated utility as potent vaccine adjuvants for a wide range of antigens in animals and humans (Cooper & Petrovsky, 2011; Gordon et al., 2012; Honda-Okubo, Saade, & Petrovsky, 2012; Larena, Prow, Hall, Petrovsky, & Lobigs, 2013; Petrovsky et al., 2013; Saade, Honda-Okubo, Trec, & Petrovsky, 2013; Cooper, Barclay, Ginic-Markovic, & Petrovsky, 2013a) and also having anticancer activity (Cooper 1993; Korbelik & Cooper, 2007). The biological importance of these isoforms accordingly lies in both *in vitro* immune activation and clinical application. A major advantage of inulin-based adjuvants for human vaccines is that they are non-inflammatory, with low reactogenicity and high human and animal safety, in contrast to more traditional adjuvants that activate inflammatory pathways (Petrovsky 2013; Petrovsky & Aguilar, 2004). This paper further explores the structural basis of these useful activities.

The chemical make-up of inulin is well known (Franck & De Leenheer, 2002). Chicory inulin comprises a family of linear (branching < 2%: De Leenheer & Hoebregs, 1994) chains of β-D-[2→1] poly(fructo-furanosyl) α-D-glucose with a range of degrees of polymerization (DP) up to 100 or more hexose moieties. Inulin solutions readily deposit particles visualized as layers of crystalline lamellae (André, Mazeau et al., 1996; André, Putaux et al., 1996; Cooper and Petrovsky, 2011; Hébette et al., 2011), each comprising inulin chains helically folded into rigid rods in parallel arrays. The arrays form broad sheets with the rods perpendicular to the lamellar plane, isoforms presumably reflecting variations in the rods' makeup.

MPI polymorphic forms/isoforms have long been recorded (Cooper & Carter, 1986; Cooper & Petrovsky, 2011; Katz & Weidinger, 1931; McDonald, 1946; Phelps, 1965). We recently described a total of seven polymorphic forms/isoforms of inulin (Cooper, Barclay, Ginic-Markovic, & Petrovsky, 2013b), comprising a fixed incremental series starting with amorphous inulin developing with increasing temperatures of treatment into forms designated alpha-1 (AI-1) → alpha-2 (AI-2) → gamma (GI) → delta (DI) → zeta (ZI) → epsilon (EI) → omega (OI); each has higher aggregate H-bonding strength than its precursor. Their biological activities also varied. Isoforms are the usual presentation of inulin polymorphic forms but differ in including increasingly longer inulin chains while the true polymorphs all have identical chain compositions; isoforms and polymorphs may share the same phenotype (thermal properties). Each was characterized either by its aqueous dissolution point or critical temperature (Tc) as identified as the point of abrupt phase shift, or by its dry melting point (MP) as measured by modulated differential scanning calorimetry (MDSC). The Tc or MP of these seven inulin isoforms/polymorphs increased in a strikingly periodic and step-wise manner, with a regular increment of 6 to 10°C or ca 2.9°C per step, respectively (Cooper et al., 2013b). This suggested that each isoform step simply reflected a regular addition of some energetic unit to a defining structure. These samples contained the entire upper range of inulin chain lengths (plus-format preparations) that obscured the minimal structure defining each isoform.

We wished to understand inulin polymorph/isoform assembly in terms of the lamellar organization of MPI. Our objectives here were to obtain a new series of isoform isolates expected to provide only that minimal definition ('monoformat' preparations), to determine the number average degrees of polymerization (DPn) of these defining structures, and to compare their X-ray diffraction characteristics with those of André, Putaux et al. (1996).

2. Materials and methods

2.1. Materials

Chicory inulin (Raftiline HP) was supplied as a single large batch in powder form by BENEO-Orafti, Tienen, Belgium. Inulin enzymically synthesized in vitro (DPn ∼20) was a gift from Fuji Nihoh Seito Corporation, Tokyo, Japan. The filtered raw material (FRM) quoted here was a 100 mg mL^{-1} solution of the raw chicory inulin as supplied, ion-exchange-and 200 nm- filtered to British/United States Pharmacopoeias compliance, prepared and monitored as described by Cooper et al. (2013b). Close temperature control is critical for this work and methods are also described in that paper. Materials were sterile and handled aseptically. All solutions and suspensions were in WFI/bic (pH ∼8: 1 mM Na bicarbonate in Water for Injection; Baxter, Sydney NSW) unless otherwise stated. Inulin concentrations were measured in the dissolved state by RI and taken as °Brix measured by a Brix-Mettler Toledo "Quick-Brix" 90 hand refractometer calibrated by the supplied standard sucrose solution, restricting sample concentrations to <200 mg mL^{-1}.

2.2. Preparation of isoforms in monoformat

We aimed for samples stable to heating at about the Tc of their plus-format analogues with similar physical properties but with evidence of little or no ability to form higher or lower isoforms. Final yields were usually rather small (<2 g). Letters in bold face type in this Section indicate the final monoformat preparation. The precipitate after thawing (7 days, 5 °C) a frozen FRM solution includes all crystallizable inulin chains, presented in a mixed alpha plus-format. Usually, this material was first heat-converted to the GI plus-format (80-100 mg mL^{-1}, 45 °C, 90 min), annealed at room temperature (RT, 20-21 °C, 1-2 weeks), adjusted to 40-50 mg mL^{-1} and heated at a temperature (39 °C) midway between the Tc of AI-2 and GI (Table 1) to extract a maximum of AI-2 chains with a minimum of GI chains.

However, the series may be entered at any point to obtain a particular isoform. The centrifuged (10-30 min, 650 g, to obtain a clear supernatant) GI precipitate resuspended to 40-50 mg mL^{-1} was first washed once at 43 °C (2 °C lower than the Tc of GI) and then at RT to supernatant RI < 2 mg mL^{-1} to yield GI in plus-format. The 39 °C extract of mixed AI chains was processed as in the next paragraph. This convert/anneal/extract/wash procedure was repeated using the known Tc values for each of the isoforms (Table 1) in turn to extract solutions expected to contain the chains of each of the isoforms in crude monoformat. All second and subsequent washes were at RT except for AI-1, which was always handled at 0 °C. Re-crystallizing becomes mandatory when extracted particles are too light to centrifuge easily. Crude monoformat extracts containing **GI** and higher chains (**DI, ZI, EI** and **OI**) were concentrated either by freeze-thaw crystallization (5 °C, 1-2 weeks) or 80%-ethanol precipitation, followed by re-crystallization and re-conversion up the series. Optimal

conversion occurs at the Tc, and other working temperatures are given in Table 1. Except for OI, the suspensions were finally converted as if to the *next higher* isoform (Table 1), which ensures that assay will reveal any higher isoform chain type contamination. The convert/anneal/extract and/or wash cycles were repeated on each isolate until the acceptance criteria (Section 3.1) were met. The incidence of sample faults described in Section 3.1 was minimized by use of a) adequate annealing times and temperatures, b) the difference between optimal extraction and washing temperatures, c) extraction concentrations (40-50 mg mL^{-1}) low enough for efficient leaching despite finite saturation concentrations, and conversion concentrations high enough (80-100 mg mL^{-1}) to lessen losses during conversion. The intent was to obtain monoformat material with the thermal characteristics of the typical plus-format isoform (Cooper et al., 2013b) in order to determine the DPn of its defining chain type.

Both alpha monoformats may be sourced either from supernatants (5-10 mg mL^{-1}) of FRM crystallized at 5 °C or from the 39 °C extracts described in the previous paragraph. Both sources were ethanol-precipitated or freeze-dried then recrystallized (100 mg mL^{-1}, 5 °C, 7-10 days) and the whole suspension converted as if to GI (90 min, 45 °C) then annealed (7-14 days, RT). AI-1 chain type was extracted (40-50 mg mL^{-1}, 25 °C, 45 min) and the centrifuged (10 min, 650 g) **AI-2** precipitate washed once at 29 °C then at RT to supernatant <2 mg mL^{-1}. The clear **AI-1** extract was dried, dissolved to 100 mg mL^{-1} and recrystallized (5 °C, 7-10 days), the whole suspension then converted as if to AI-2 (90 min, 32 °C) and annealed (7-14 days, 5 °C), then washed at 0 °C to supernatant <2 mg mL^{-1}. A single exception was a solution of synthetic inulin (DPn 20), which spontaneously precipitated material with the properties of **AI-1** monoformat (100 mg mL^{-1}, 7 days and 5 °C). This was purified as for other AI-1 precipitates.

2.3. DPn assay

^{1}H NMR spectra were recorded on a Bruker Avance III 600 at 600 MHz for ^{1}H (Barclay, Ginic-Markovic, Johnston, Cooper, & Petrovsky, 2012). The integral of the glucose anomeric peak at 5.44 ppm (see Supplementary Data) was set to 1 to calibrate a spectrum and its ratio to the combined integral of all other resonances of inulin (= *X*) provided a measure of the average number of fructose units in the chain = $(X - 6)/7$ = (DPn -1). One-dimensional spectra were processed as described by Cooper et al. (2013b). Duplicate ^{1}H NMR spectra were each analysed three times to give an overall average for (DPn - 1), adding 1 to include the terminal glucose.

2.4. X-ray diffraction

XRD data collection was performed at room temperature on a Bruker D4 Endeavor diffractometer with Co Kα radiation (1.7902 Å) at 30 kV and 20 mA. Diffraction patterns were collected with θ/2θ geometry from 5 to 80° 2θ at 0.02° 2θ increments with a rotating sample stage to ameliorate any possible preferred orientation effects. No sample preparation was undertaken due to the inherent fine particle size of the sample (< 2 μm).

3. Results

3.1 Criteria for acceptance of monoformat isolates

Samples for DP analysis are shown able to form mainly only one isoform by all of four criteria: provenance (isolation context, Section 2.2), temperature-solubility properties measuring both OD_{700} at <2 mg mL^{-1} and RI at >20 mg mL^{-1} (procedures described in Fig. 1), and failure to convert to the next higher isoform. Non-compliance of the supposed monoformat is detected by the shape of the OD_{700} and temperature solubility curves, which may appear a frank mixture of two curves or covertly biphasic, with a high solubility at its lower assay temperature (Table 1) and/or a high insolubility at its higher assay temperature; alternatively the apparent Tc is not within the limits found by Cooper et al. (2013b). All of these may indicate undesired chain type contamination. Inadequate heat-conversion or annealing may appear similar. Acceptable OD_{700} and solubility curves are shown in Fig.1 and the prime criterion for compliance is the close similarity of such curves both before and after attempted conversion/annealing to the next higher isoform. Complying samples are presumed to be largely free (< 5 % w/w) of inulin chain types irrelevant to the minimal defining structure of the majority isoform and are accepted for assay as monoformat preparations.

Each isoform type presents its own complexities. Un-annealed plus-format samples, presumably stabilized by the presence of longer chains, are less easily washed away than their un-annealed equivalent in monoformat, which are usually quite unstable in water at 20°C. Adequate annealing of the monoformat samples is crucial. Annealed AI-1 monoformat is unstable at 20 °C (half-life 7 - 10 min at 2 mg mL^{-1}) but stable at 0 °C; AI-2 is stable to washing at 20-22 °C, when AI-1 chain type is completely removed. Annealed GI monoformat isolation is relatively straightforward. Annealed DI, ZI and EI monoformats have closer thermal properties and so are more difficult to separate. In contrast, the highest isoform (OI) misleadingly seems easy to isolate by robust heating and washing. In fact, as it includes the entire upper range of chain lengths, its broader range of DP and Tc values requires more replicate samples to achieve stable average values (Section 3.2).

3.2. Properties of monoformat isolates

Fig. 1 shows the OD_{700} and RI curves defining the thermal properties of typical, well-annealed, acceptable isoform monoformat preparations. These curves are very like those similarly defining the analogous plus-format preparations (Cooper et al., 2013b) and their Tc and DPn values are compared in Table 2. The DPn values increase by a regular 6 hexose units, always with an extra pair, following the progression 6N + 2. The Tc values themselves are close to those of the analogous plus-format samples except that the two alpha monoformats have significantly lower Tc (OD_{700}) values. Coefficients of variation (CV) of replicate Tc values are < 2%, comparable to those of the plus-format isoform samples. The variability of the DPn values is also fairly low, three isoform types having a CV of < 3%. The SD of the mean DPn value of each isoform is generally similar to those of its component individual DPn values, which are themselves averages of 6 replicate ratio measurements (Barclay et al., 2012) plus the terminal glucose. When samples are listed in

order of increasing Tc (RI) value their individual Tc (OD) and DPn values do not vary in the same sequence (data not shown) and so any variation seems unlinked.

The considerable variability among the DPn values of OI presumably reflects the wider range of chain lengths expected, as OI resembles a plus format in that it includes a range of chains longer than those minimally defining the omega phenotype. An excess of longer chains could still therefore obscure the minimum structure of OI. Surprisingly, the DPn of individual OI samples does not relate closely to their Tc. To explore this, three samples of OI are prepared from a sample of DPn 60.1 by attempted removal of lower DP material on washing at 79 °C, 82 °C and 84 °C respectively, the amounts removed indicating that the residues should comprise the top 60%, 50% and 20% of longer chains. In fact, the DPn is only increased to 63.5, 65.0 and 65.5 respectively, so it seems any longer chains are in a small minority. Again the Tc values do not change in parallel but actually decrease. Like the plus-format isoforms, individual Tc values vary independently within a common range (Fig. 2B), the common factor being their isoform cluster: they seem linked by a basic common structure. Such minor variation likely reflects cumulative experimental error.

The DPn values are compared with isoform type in Fig. 2A, plotting the variable actually measured (DPn - 1) against isoform type. This ignores the terminal glucose. The minimum number of putative unit cells (helix turns; André, Mazeau et al., 1996) is estimated in Fig. 2A as (DPn -1)/6 to the nearest integer and is returned to in Section 4. The quantitative repeats seen in the Tc values and MDSC melting points of the plus-format isoforms (Cooper et al., 2013b) are mirrored for the monoformat isolates in Fig. 2A, namely an almost precisely consistent increase of 6 fructose residues per isoform (12 for OI). The mean interval (Table 2), is 6.016 ± 0.080 SD (CV = 1.33) fructose residues per incremental unit.

The (DPn - 1) progression of Fig. 2A does not correspond to the simple formula 6N (N = unit cells) but to 6N + 1, i.e. each isoform contains 1 more fructose residue per chain than expected (discussed in Section 4). While the difference is small (5% and decreasing up the series) it is consistent throughout, and the two data sets (observed (DPn -1) and expected 6N) are significantly different ($p = 0.00057$, t test). The linear trend line for the (DPn -1) data set created by the software (MS Excel 2007™) and illustrated in Fig. 2A is indistinguishable from the theoretical curve 6N + 1. The average ± SD ‘excess’ of fructose residues per isoform type is 1.09 ± 0.495, so the observed excess is on average > 2 × its SD ($p < 0.05$). Like the Tc values of the plus format isoforms, the Tc values of the monoformat isolates (Fig. 2B) show a step-wise progression and are clustered around a mean value with no overlap. The diversity of inulin chain lengths in the monoformat samples will be much less than in the earlier plus-format samples but we expect that significant size distribution will be retained.

A plot of Tc values against monoformat isoform type and calculated unit cell contents shows a different aspect (Fig. 2C). The polynomial trend-lines for Tc (OD) and Tc (RI) are indistinguishable and follow a non-linear relation typical of diminishing marginal returns, where each additional unit cell increases the overall Tc (a measure of aggregate energetic content) by progressively smaller amounts. A similar but less marked effect is seen with the plus-format isoform Tc values (Cooper et al., 2013b), where presumably the presence of

longer chains provides more thermal stability particularly for AI-1 and AI-2. The Tc values are aqueous phase-shift points, where water interactions will be important in the H-bond rupture involved. Fig. 2C is in sharp contrast to the dry phase-shifts revealed by MDSC analyses, which show a strictly linear relation between MP and (plus-format) isoform type at much higher temperatures (Cooper et al., 2013b).

Two anomalies need mention. Firstly, Table 2 and Fig. 2 have no stable member of DPn ca 56 (9 unit cells) between EI and OI. It was not found in a systematic search (Cooper et al., 2013b) and slow heating (conversion) of EI produces only OI. Also the regular relation between isoform type and both Tc and MP fail to leave a gap for such a member. Finally, any contaminating chain type found in EI monoformat isolates could only form OI (data not shown). Thus such an isoform seems not to exist. Secondly, as its name implies, no higher isoform than omega inulin was found. These two anomalies may be linked by the common factor of diminishing marginal returns (Fig. 2C), where further chain length investment fails to give sufficient energetic return to stabilize the missing entities.

With the exception of these anomalies, Fig. 2 summarizes the finding that the inulin isoform series arises from the repeated addition of a constant structural feature consisting of 6 fructose residues per chain

3.3 X-ray diffraction patterns and crystal structure

André, Mazeau et al. (1996) described one unit cell of single crystals of inulin (DPn ca 20) based on electron and X-ray diffraction analysis (André, Putaux et al. (1996). This unit cell comprised one turn of each of two antiparallel helices, each turn made up of 6 fructose residues and in the case of the fully hydrated form with one molecule of water of crystallization for each fructose. A specific web of hydrogen bonds connected the chains and some water molecules, and the overall structure was semicrystalline in nature. The presence of crystalline material here is confirmed in examples of all the inulin monoformat isoforms by their X-ray diffraction patterns (Fig. 3). Those plus-format preparations tested display similar patterns (data not shown). All patterns turn out to be indistinguishable from each other and from the *d*-spacings and intensities described by André, Puteau et al. (1996). The monoformat isoforms shown are AI-1, AI-2, GI, DI, ZI, EI and OI, comprising mean chain lengths of 3, 4, 5, 6, 7, 8 and 10 groups of six fructose units respectively, in each case with the terminal glucose and an extra fructose (Section 3.2). The broad peaks suggest that no sample has a high degree of crystallinity.

4. Discussion

The very regular increases in the Tc and MP values of the plus-format inulin isoform series, plus an increasing trend in their DPn values, led us to suggest that the definitive structure of each isoform had increased by one full energetic unit (Cooper et al, 2013b). An attractive candidate for the energetic unit was the unit cell of André, Mazeau et al. (1996), deduced to comprise one complete turn of 6 fructose residues per chain in each of two anti-parallel helical chains. A clear quantitative relation is seen here when irrelevant chains are excluded and each monoformat isoform can indeed be shown to comprise 6 fructose residues per chain more than its precursor. Thus the ‘energetic unit’ equates to these 6 fructose units. The

exception of omega inulin, 12 fructose units more, is discussed in Section 3.2. Despite this, the repeated addition of 6 fructose units did not change the X-ray diffraction pattern. Thus each added 6-unit group has the same pattern, which is the same as in the inulin crystal (André, Putaux et al, 1996). That is, each energetic unit has the same structure as one unit crystal cell. It was unexpected that each isoform consistently involved an extra fructose residue, following the overall (DPn - 1) progression 6N + 1 rather than the expected 6N. We are currently exploring the role of this extra fructose and of the unit cell progression in inulin particle structure by molecular modelling.

5. Conclusions

We conclude that the isoforms differ by repeated additions of one unit cell to critical components of the crystalline portions of the inulin particle. In the case of the monoformat preparations this appears to be the physical length of chains comprising the helically folded rods in the lamellar arrays. For the plus-format isolates or for true polymorphic forms where chain lengths do not differ, the differences presumably lie in the lengths of regions that can assume the H-bonding conferring the particular thermal stability observed for each isoform. However, the abundant presence of water molecules means that theoretical dimensions for lamellae calculated from these parameters do not necessarily correspond to those existing in the inulin particles.

Supplementary Material

Refer to Web version on PubMed Central for supplementary material.

Acknowledgments

We thank Dr Doug Taupin for invaluable support throughout the course of these studies, and Daniel Whateley and Timothy Jose for excellent technical assistance. We also thank Fuji Nihoh Seito Corporation, Tokyo, Japan, for a generous gift of synthetic enzymic inulin. P.C. is an Emeritus Visiting Fellow of the Australian National University Medical School and of the John Curtin School of Medical Research, ANU, Canberra, Australia.

Funding: This work was supported in whole or in part by Federal funds from the National Institute of Allergy and Infectious Diseases, National Institutes of Health, US Department of Health and Human Services (HHSN272200800039C and U01AI061142). The content is solely the responsibility of the authors and does not necessarily represent the official views of the National Institute of Allergy and Infectious Diseases or the National Institutes of Health. This work was also supported by The Australian Research Council through a Linkage Grant (LP0882596) and a LIEF Grant (LE0668489).

References

André I, Mazeau K, Tvaroska I, Putaux JL, Winter WT, Taravel FR, Chanzy H. Molecular and crystal structures of inulin from electron diffraction data. Macromolecules. 1996; 29:4626–4635.

André I, Putaux JL, Chanzy H, Taravel FR, Timmermans JW, de Wit D. Single crystals of inulin. International Journal of Biological Macromolecules. 1996; 18:195–204. [PubMed: 8729031]

Barclay T, Ginic-Markovic M, Cooper P, Petrovsky N. Inulin - a versatile polysaccharide with multiple pharmaceutical and food chemical uses. Journal of Excipients and Food Chemistry. 2010; 1:1–24.

Barclay T, Ginic-Markovic M, Johnston MR, Cooper PD, Petrovsky N. Analysis of the hydrolysis of inulin using real time ^{1}H NMR spectroscopy. Carbohydrate Research. 2012; 352:117–125. [PubMed: 22464225]

Cooper, PD. Solid-phase activators of the alternative pathway of complement and their use in vivo. In: Sim, RB., editor. Activators and inhibitors of complement. Dordrecht (Netherlands): Kluwer Academic Publishers; 1993. p. 69-106.

Cooper, PD.; Barclay, TG.; Ginic-Markovic, M.; Petrovsky, N. Gamma ray sterilization of delta inulin adjuvant particles (AdvaxTM) makes minor, partly reversible structural changes without affecting adjuvant activity. Vaccine (2013). 2013a. http://dx.doi.org/10.1016/j.vaccine.2013.11.105

Cooper PD, Barclay TG, Ginic-Markovic M, Petrovsky N. The polysaccharide inulin is characterized by an extensive series of periodic isoforms with varying biological actions. Glycobiology. 2013b; 23:1164–1174. [PubMed: 23853206]

Cooper PD, Carter M. Anticomplementary action of polymorphic 'solubility forms' of particulate inulin. Molecular Immunology. 1986; 23:895–901. [PubMed: 3796631]

Cooper PD, Petrovsky N. Delta inulin: a novel, immunologically active, stable packing structure comprising β-D-[2→1] poly(fructo-furanosyl) α-D-glucose polymers. Glycobiology. 2011; 21:595–606. [PubMed: 21147758]

De Leenheer L, Hoebregs H. Progress in the elucidation of the composition of chicory inulin. Starch. 1994; 46:193–196.

Franck, A.; De Leenheer, L. Inulin. In: Vandamme, EJ.; De Baets, S.; Steinbüchel, A., editors. Biopolymers vol 6 Polysaccharides II: Polysaccharides from eukaryotes. Vol. Chapter 14. Berlin: Wiley-VCH Verlag GmbH; 2002. p. 439-479.

Gordon DL, Sajkov D, Woodman RJ, Honda-Okubo Y, Cox MM, Heinzel S, Petrovsky N. Randomized clinical trial of immunogenicity and safety of a H1N1/2009 pandemic influenza vaccine containing Advax polysaccharide adjuvant. Vaccine. 2012; 30:5407–5416. [PubMed: 22717330]

Hébette CL, Delcour JA, Koch MHJ, Booten K, Reynaers HL. Crystallization and melting of inulin crystals. A small angle X-ray scattering approach (SAXS). Polimery. 2011; 56:645–651.

Honda-Okubo Y, Saade F, Petrovsky N. Advax™, a polysaccharide adjuvant derived from delta inulin, provides improved influenza vaccine protection through broad-based enhancement of adaptive immune responses. Vaccine. 2012; 30:5373–5381. [PubMed: 22728225]

Katz JR, Weidinger A. Polymorphism of substances of high molecular weight. II. Amorphous and crystalline inulin. Receuil des Travaux Chimiques des Pays-bas et de la Belgique. 1931; 50:1133–7. Abstract only available.

Korbelik M, Cooper PD. Potentiation of photodynamic therapy of cancer by complement: the effect of gamma-inulin. British Journal of Cancer. 2007; 96:67–72. [PubMed: 17146472]

Larena M, Prow NA, Hall RA, Petrovsky N, Lobigs M. JE-ADVAX vaccine protection against Japanese encephalitis mediated by memory B cells in the absence of CD8+ T cells and pre-exposure neutralizing antibody. Journal of Virology. 2013; 87:4395–4402. [PubMed: 23388724]

McDonald EJ. The polyfructosans and difructose anhydrides. Advances in Carbohydrate Chemistry. 1946; 2:253–277.

Petrovsky N. Vaccine adjuvant safety: the elephant in the room. Expert Reviews in Vaccines. 2013; 12:715–717.

Petrovsky N, Aguilar JC. Vaccine adjuvants: current state and future trends. Immunology and Cell Biology. 2004; 82:488–496. [PubMed: 15479434]

Petrovsky N, Larena M, Siddharthan V, Prow NA, Hall RA, Lobigs M, Morrey J. An inactivated cell-culture Japanese encephalitis vaccine (JE-ADVAX) formulated with delta inulin adjuvant provides robust heterologous protection against West Nile encephalitis via cross-protective memory B cells and neutralizing antibody. Journal of Virology. 2013; 87:10324–10333. [PubMed: 23864620]

Phelps CF. The physical properties of inulin solutions. Biochemical Journal. 1965; 95:41–47. [PubMed: 14333566]

Saade F, Honda-Okubo Y, Trec S, Petrovsky N. A novel hepatitis B vaccine containing Advax, a polysaccharide adjuvant derived from delta inulin, induces robust humoral and cellular immunity with minimal reactogenicity in preclinical testing. Vaccine. 2013; 31:1999–2007. [PubMed: 23306367]

Abbreviations

AI-1	alpha-1 inulin
AI-2	alpha-2 inulin
BP	British Pharmacopoeia
DI	delta inulin
EI	epsilon inulin
FRM	filtered raw material (Methods)
GI	gamma inulin
MPI	microparticulate inulin
NA	not applicable
ND	not determined
OI	omega inulin
PBS	phosphate buffered saline
RI	refractive index
RT	room temperature (20 - 21°C)
Tc	critical temperature
USP	United States Pharmacopoeia
WFI/bic	1 mM Na bicarbonate solution in Water for Injection
ZI	zeta inulin

Highlights

Cooper et al. Inulin isoforms

- New ‘monoformat’ isolates of all seven inulin isoforms had limited chain lengths
- Monoformat isolates can only make the single isoform defined by these chains
- Isoform type and properties increased in regular steps with every 6 fructose units
- X-ray diffraction patterns of the isoforms and inulin crystals were all identical
- We conclude inulin isoforms differ by regular increases of one crystal unit cell

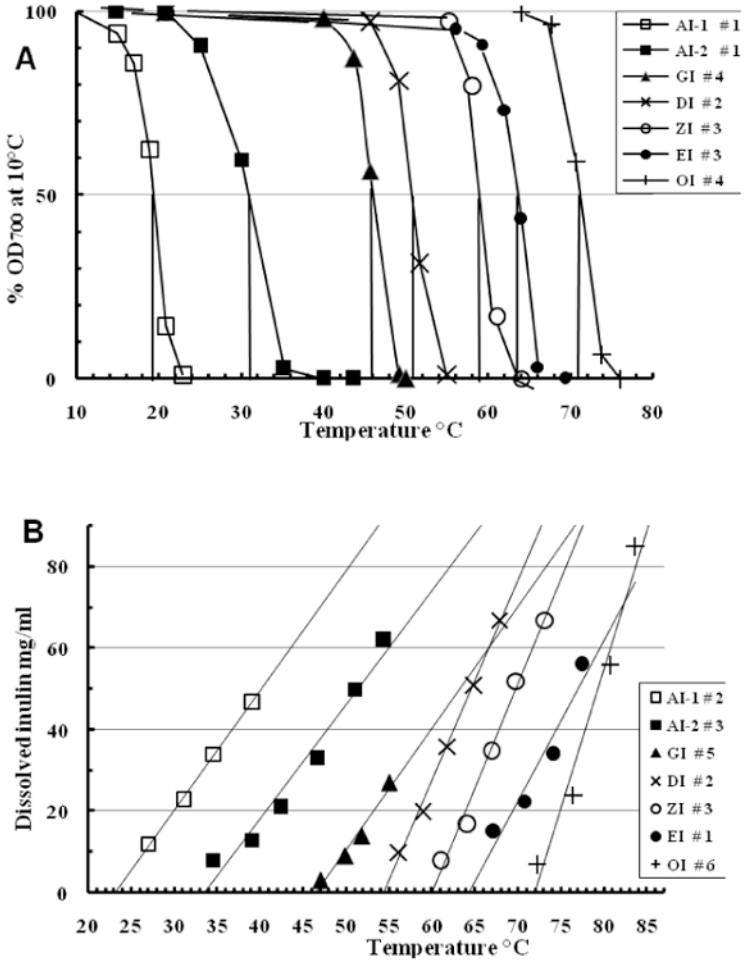

Fig. 1.

Comparisons of thermal properties of typical monoformat isoform isolates satisfying the monoformat criteria, showing conformity with the plus-format series (Cooper et al., 2013b). (**A**) OD_{700} thermal transition curves. Dilutions in PBS at 0.5 mg mL^{-1} are progressively heated and the OD_{700} of each measured after equilibration at each indicated temperature. (**B**) Temperature solubility curves. Sealed Eppendorf centrifuge tubes containing 0.5 mL of isoform suspensions at 50-100 mg mL^{-1} are fully immersed in water baths at the indicated temperatures for 15 min and then centrifuged (4 min, 18,000g) to measure supernatant RI. The linear trend-lines created by the application (MS Excel 2007™) are extrapolated to zero supernatant content. Legends show sample numbers of Table 2.

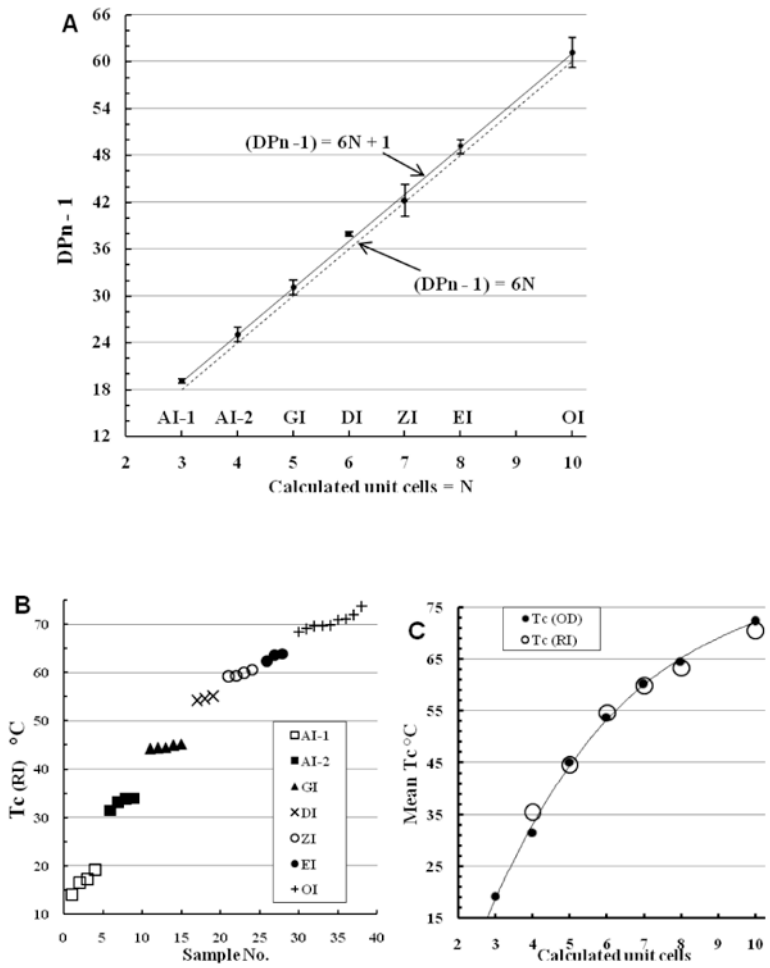

Fig. 2.

Relation of DPn to monoformat isoform type (Table 2). (**A**) Mean (DPn - 1) values plotted against isoform type and unit cells calculated as DPn/6 (nearest integer). Error bars show ± standard error. The dashed line shows the expected progression 6N, while the solid line shows the linear trend line (MS Excel™ 2007) of the observed (DPn -1) progression. (**B**) Tc (RI) values of the monoformat preparations arranged in increasing order. (**C**) Mean Tc plotted against calculated unit cells.

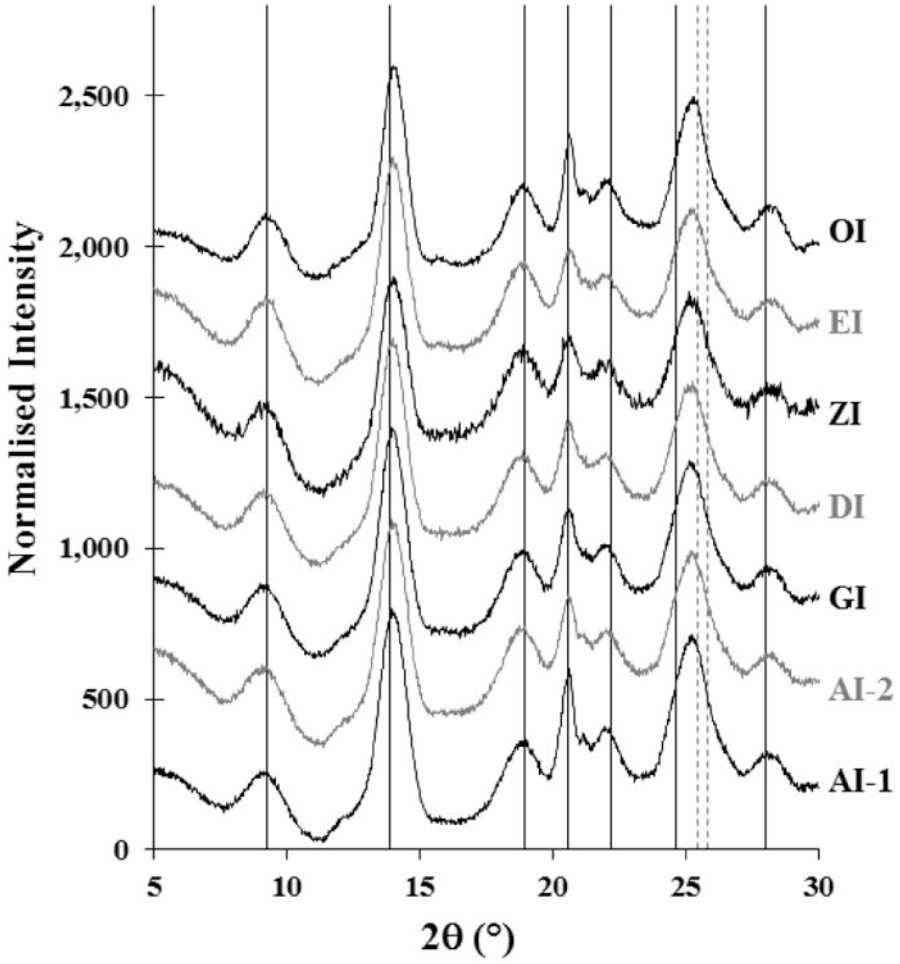

Fig. 3.

X-ray diffraction patterns of examples of all monoformat isoforms, displaced vertically to separate them. The seven vertical solid lines are at 2θ values calculated (Bragg's law) from the d_{obs} spacings of the monohydrate inulin crystal reported by André, Putaux et al. (1996, Table 4: *hkl* designations 101, 111/201, 202/112, 020/310, 311/021, 400/220, and 222/402, of which six values are composites of more than one diffraction peak). The peak at ∼25.5°2θ is taken to be a composite of d_{obs} spacings 400/220, and 221/411 (dashed lines) from electron diffraction data in Table 3 of that paper.

Table 1

Significant temperatures (°C) for monoformat inulin isoforms

	AI-1	AI-2	GI	DI	ZI	EI	OI
Tc/Conversion[a]	17	32	45	54	60	64	71
Anneal[b]	5	20	20	37	37	45	45
Extract[c]	25	39	49	57	62	68	N/A
1st wash	0 [d]	29	43	52	58	62	68
Assay (OD_{700})[e]	10	21	39	49	55	60	68

[a] 80-100 mg mL^{-1}, 90 min;

[b] 7-14 days;

[c] 40-50 mg mL^{-1};

[d] All washes are at 0 °C;

[e] T °C to distinguish that isoform from the next lower isoform.

Table 2
Properties of inulin monoformat isoform isolates

	Isoform type	Tc °C (OD)	Tc °C (RI)	DPn
AI-1	mean ± SD (CV)	16.7 ± 2.15 (12.8)	23.0 (ND) [a]	20.1 ± 0.52 (2.6)
(4)[b]	range	14.0 - 19.2	ND	19.6 - 20.7
	plus-format	23	24.5	
AI-2	mean ± SD (CV)	29.0 ± 1.48 (4.4)	33.1 ± 1.12 (3.06)	26.0 ± 1.9 (7.1)
(4)	range	27.5 - 31.0	31.5 - 34.0	25.1 - 28.7
	plus-format	34.0	34.0	
GI	mean ± SD (CV)	45.1 ± 0.98 (1.8)	44.7 ± 0.42 (0.94)	32.1 ± 2.08 (6.5)
(5)	range	44.5 - 46.3	44.2 - 45.2	29.1 - 34.2
	plus-format	44.8	45.0	
DI	mean ± SD (CV)	53.7 ± 1.04 (1.9)	54.7 ± 0.45 (0.8)	38.9 ± 0.51 (1.3)
(3)	range	52.5 - 54.3	54.3 - 55.2	38.5 - 39.5
	plus-format	52.5	52.8	
ZI	mean ± SD (CV)	60.1 ± 0.90 (1.5)	59.9 ± 0.65 (1.1)	43.2 ± 4.09 (9.5)
(4)	range	59.3 - 60.9	59.3 - 60.7	38.3 - 47.1
	plus-format	57.0	57.7	
EI	mean ± SD (CV)	64.5 ± 0.46 (0.7)	63.3 ± 0.87 (1.4)	50.1 ± 1.45 (2.9)
(3)	range	64.0 - 64.8	62.3 - 64.0	48.7 - 51.6
	plus-format	65.0	64.2	
OI	mean ± SD (CV)	72.2 ± 2.35 (3.3)	70.6 ± 1.63 (2.3)	62.2 ± 5.65 (9.1)
(9)	range	69.1 - 75.5	68.5 - 73.8	50.4 - 68.8
	plus-format	71.0	72.0	

[a] ND = not determined, samples too small;

[b] No. of replicate samples tested